International Journal of Technology (2015) 2: 160-168
ISSN 2086-9614

CIRCULAR-POLARIZED PROXIMITY-FED TIP-TRUNCATED TRIANGULAR SWITCHABLE ARRAY FOR LAND VEHICLE MOBILE SYSTEM

Basari[1*], Josaphat Tetuko Sri Sumantyo[2]

[1]*Department of Electrical Engineering, Faculty of Engineering, Universitas Indonesia, Kampus UI Depok 16424, Indonesia*
[2]*Center for Environmental Remote Sensing (CEReS), Chiba University 1-33, Yayoi, Inage, Chiba 263-8522 Japan*

(Received: February 2015 / Revised: April 2015 / Accepted: April 2015)

ABSTRACT
This paper proposes a compact, circularly polarized (CP), tip-truncated, triangular patch array developed for a land vehicle mobile system for mobile satellite communications. The array is constructed by three patches so that its beam pattern can be switched in three 120°-coverage beams in the azimuth plane with minimum gain requirement at a fixed point of the elevation angle. With this pattern, data communications with a large geostationary satellite can be achieved. The targeted gain is set to be 5 dBic at 48° of the looking angle from the satellite in the Kanto area. The patches are fed with a proximity feed technique because of its simplicity and easier installation on the vehicle. The array performance is numerically analyzed with the method of moment to clarify the array characteristics. Measurement results are provided to validate the simulated results. The results show that the array meets the specifications at the targeted looking angle of 48° when the gain is more than 5-dBic for each three-selectable beams in the azimuth plane.

Keywords: Circularly polarized triangular patch array; Land vehicle mobile system; Proximity feeding; Switchable beam

1. INTRODUCTION

The Japanese Geostationary Satellite, called the Engineering Test Satellite VIII (ETS-VIII), was launched by the Japan Aerospace Exploration Agency (JAXA) in 2006. The ETS-VIII conducts experiments on mobile satellite communications in S-band applications, especially to support technological development of multimedia communications, including voice and images for land mobile systems (Jang et al., 2002). This paper proposes a compact, satellite-track, tip-truncated, triangular patch array antenna. The targeted minimum gain of the antenna is set to 5 dBic at an elevation angle of 48° for applications having a data rate of a few hundred kilobit per second in the surrounding Kanto area. The antenna is designed to be thin, compact, and with a simple construction in order to be easily installed on a small vehicle's roof (Ishihara et al., 2002). Moreover, the array is expected to be applicable for emergency services (in particular for disaster information systems).

A mobile land vehicle satellite system needs an antenna model that can respond to the changing direction of the vehicle. Antennas that are able to meet such antenna requirements and which are currently documented in scientific articles include the conical beam antennas, such as the

[*] Corresponding author's email: basyarie@eng.ui.ac.id, Tel. +62-21-7270078, Fax. +62-21-7270077
Permalink/DOI: http://dx.doi.org/10.14716/ijtech.v6i2.946

wire quadrifilar or bifilar helix (Kilgus, 1975; Yamaguchi & Ebine, 1997), the drooping dipole (Gatti & Nybajjen, 1990) or patch antennas with a higher mode operation (Nakano et al., 1990; Ohmine et al., 1996), and tracking-based antennas (Ito et al., 1988). The key feature in the former antennas is that satellite tracking is not required because the radiation pattern is an omnidirectional pattern in the azimuthal plane. However, due to the typically low gain of up to 4 dBi (Fujimoto & James, 1994; Ohmori et al., 1998), a very high-gain satellite antenna is required. Since we require a targeted gain of more than 5 dBi in all azimuth angles (Table 1), using the aforementioned antenna types will not meet the target. Hence, we chose a satellite tracking-based antenna for this research.

Table 1 Specification and target of the antenna

Specification	
Frequency band	2500.5 to 2503.0 MHz (for reception)
Polarization	left-handed circular polarization
Target	
Elevation angle (*El*)	$48° \pm 10^{o}$
Azimuth angle (*Az*)	0° to 360°
Gain	≥5 dBic
Axial ratio	≤3 dB

Most recent antenna designs for mobile vehicle systems are cumbersome due to the mechanical beam steering that makes their system too bulky. In addition, mobile vehicle systems have a high power consumption and low tracking speed (Kuramoto et al., 1988; Huang & Densmore, 1991; Bayer et al., 2014). Another system solution is by using a phased array that employs electronic beam steering (Alonso et al., 1996; Vaccaro et al., 2010), but the existence of phase shifters makes this costly because of the large number of phase shifters required. Again, beam squinting may occur between the transmitting and receiving directions.

In order to reduce the bulkiness of the antenna design, a new structure of a planar array antenna is proposed without any phase shifters. This results in a light and small antenna that is reliable and has relatively high-speed tracking. In this paper we discuss the realization of the proposed antenna.

2. SPECIFICATION, TARGET, AND ARRAY STRUCTURE

Table 1 shows the specifications and target of the required antenna for mobile satellite communications in ETS-VIII applications. The antenna is designed for reception purposes. A slim miniaturized antenna designed for data communication at a few hundred kilobit per second is designed and numerically simulated by using Method of Moment (MoM; Ansoft Ensemble) software. It assumes that 5 dBic of antenna gain is required. The measurement is conducted as though it is operating in the Tokyo area, so the elevation angle *El* has a 48° target. In the initial design, the center frequency for a single patch is 2.5025 GHz. Then, the antenna is sequentially arranged in an array configuration in order to make a simple switch technique for satellite tracking. The antenna is fabricated on a dielectric substrate with relative permittivity $\varepsilon_r = 2.17$ and $\tan\delta = 0.00085$. It is then measured in an anechoic chamber to confirm the simulated results.

Figure 1 shows the structure of a tip-truncated triangular patch array. The proposed array consists of three tip-truncated triangular patch elements. This configuration is expected to have a small size when it is installed on the vehicle's roof. Each patch is fed by a single proximity microstrip with a width *w* of 3.0 mm; thus, a thin and simple structure is achieved. This single proximity feeding is able to generate left-handed circular polarization (LHCP) by shifting a microstrip line l_f to the left of the center of the element. Right-handed circular polarization is also able to be realized by putting the microstrip line on the opposite side. This feeding type is designed to obtain a simple structure and easy fabrication and improves the previously proposed antenna (Sri Sumantyo et al., 2004a, 2004b, 2005a).

In previous studies, several types of circularly polarized triangular antennas were developed by using the probe-feed types (Lu & Wong, 2002; Suzuki et al., 1987; Garg et al., 2001; James & Hall, 1989; Kumar & Ray, 2003). The probe-feed type is performance sensitive compared to the co-planar line or proximity-feed type, particularly during the fabrication process. Hence, by using proximity feeding, as shown in Figure 1, the antenna with tip-truncated triangular patches has a stable construction, especially compared to earlier developed antennas (Sri Sumantyo et al., 2005a).

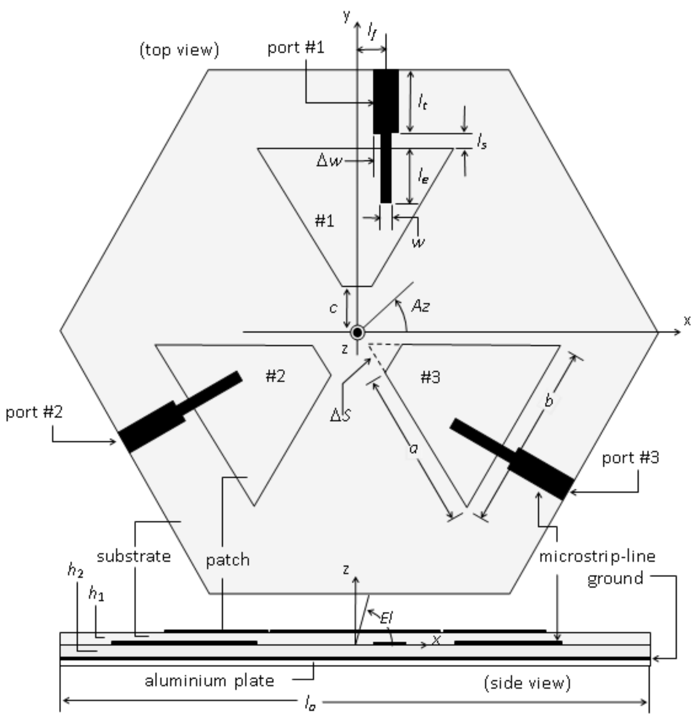

Figure 1 Structure of the array antenna

MoM-based software is used to simulate an array model with an infinite ground plane. The total thickness of the array is 1.6 mm and consists of two substrate layers, i.e., upper and lower layer, denoted in Figure 1 by h_1 and h_2, respectively, where each thickness is 0.8 mm. The length of the proximity microstrip line under patch l_e is 14 mm and under patch l_s is 5 mm. The transformer, with l_t = 10 mm and Δw = 0.5 mm, is adjusted to get a 50-Ω impedance matching. A small area on the triangular tip Δ*s* (10 mm^2) is cut to ensure a good circular polarization. Lastly, the array is fed by a SMA connector on the edge of the substrate. The detail parameters of the proximity microstrip-line are l_f = 9 mm (see Figure 1). The patch size is optimized to obtain good resonant frequency characteristics. Ultimately, the patch size *a* = 49.4 mm and *b* = 52.8 mm is obtained. By considering the coupling and axial ratio characteristics, a length *c* = 10 mm is set for this array.

Figure 2 depicts a fabricated, tip-truncated, triangular patch array. The array operates a beam-switching mechanism to electronically track the satellite. It is realized by switching one of the radiating elements off, as shown in Figure 3. The array elements that are excited (switched on) are called "active" elements. With two active elements, mutual coupling between elements leads to a different phase shift and current distributions on each element due to their spatially different position; thus, the beam will be directed in a different direction. Two active elements will generate a shifted beam by –90° in the azimuthal plane from the switched-off element for an LHCP array. Hence, when element 3 (#3) is off, the beam of the array is directed toward the azimuth angle *Az* = 240° (in Figure 10, beam no. 3 in the graph). In this array, we can generate three differently directed beams. The other two beams are also generated by switching element #1 or #2 off to make the other two differently directed beams. The theoretical mechanism of the aforementioned beam generation of the array (Figure 3) is analyzed by using a point-source model that was reported in Sri Sumantyo and Ito (2006).

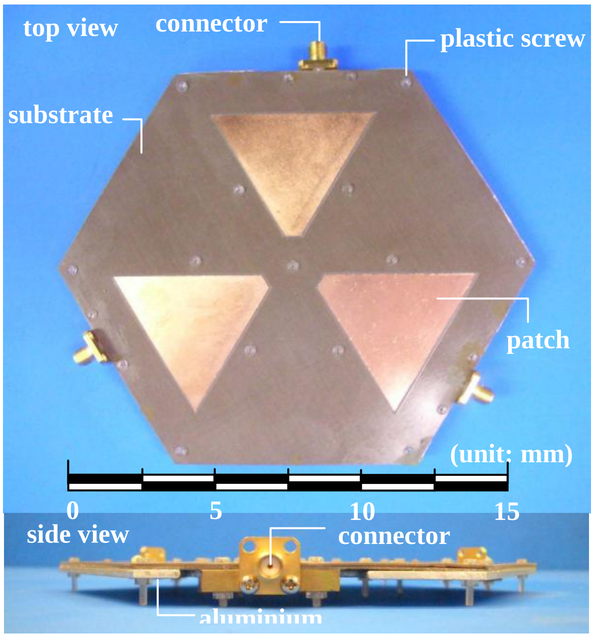

Figure 2 Fabricated antenna

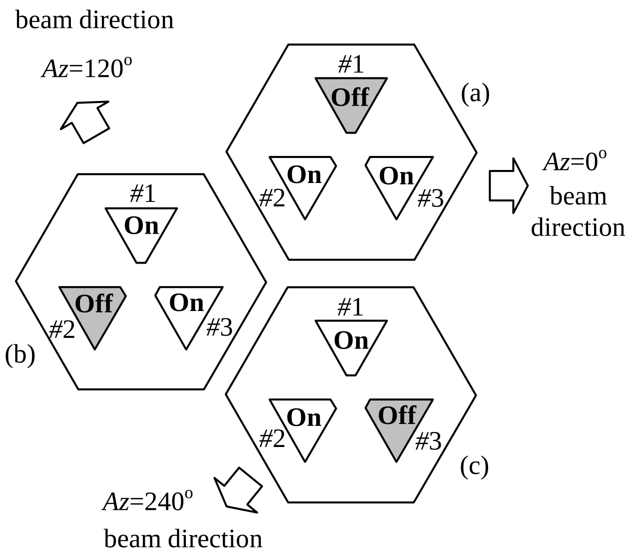

Figure 3 Switching mechanism of the developed antenna: (a) patch #1 off; (b) patch #2 off; (c) patch #3 off

3. RESULTS AND DISCUSSION

When the antenna is arranged in an array configuration, the influence of the distance between the triangular patch apex (edge of the truncated tip) and the center of the array (symbolized by *c* in Figure 1) is investigated, including the effect of ground size. For the compact size and matched target, *c* is simply varied from 5 to 15 mm. The measurement results are shown in Figures 4 and 5. The analysis is addressed in the following paragraph.

The gain against the azimuth angle *Az* (when #3 is off) for *c* = 5, 10, and 15 mm at *El* = 48° is depicted in Figure 4. The 5-dBic beamwidth for *c* = 5, 10, and 15 mm is 116°, 124°, and 128°, respectively. The main beam slightly decreases when *c* is increased. The saddle-like main beam is generated by the turned-on patches, which are separated by more than 0.6 λ of distance. The figure also shows that a higher side lobe is obtained by increasing *c*. The 5-dBic coverage of the main beam for *c* = 5 and 10 mm satisfies the target, i.e., it is wider than at least 120° coverage to meet 360° coverage by the three different beams, as previously presented in Section 2.

Figure 4 also provides information about the axial ratio performance against *Az*. The 3-dB axial ratio beamwidth is 139°, 146°, and 147° for *c* = 5, 10, and 15 mm, respectively. The 3-dB axial ratio beamwidth for *c* = 15 mm is the widest compared to the others. However, its axial ratio beamwidth shifts to the right compared to the 5-dBic gain beamwidth.

The gain performance versus elevation angle (*El*) is shown in Figure 5. The increase in *c* results in the peak gain having a higher elevation angle. The 5-dBic beamwidth coverage is by 41°, 42°, and 41° for *c* = 5, 10, and 15 mm, respectively, and the main beam is directed to *El* = 61°, 63°, and 65°, respectively. The increase in *c* will increase the side lobe level due to increasing the size of the ground plane (Sri Sumantyo et al., 2005b).

Figure 5 also describes the axial ratio performance in the *El*-plane. The 3-dB axial ratio coverage for *c* = 5, 10, and 15 mm is 71°, 72°, and 75°, respectively. The nearer array configuration will generate much coupling among the elements, so the characteristics of the array changes significantly.

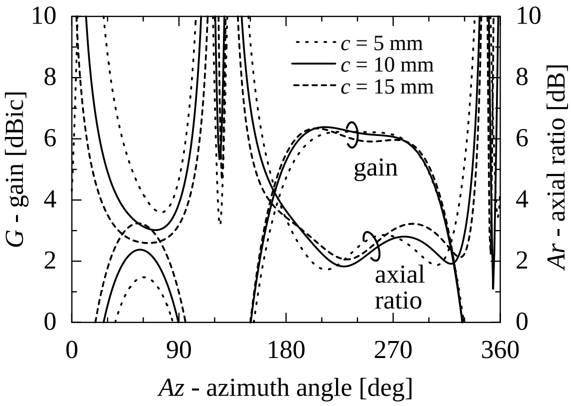

Figure 4 Gain and axial ratio versus azimuth angle (patch #3 off)

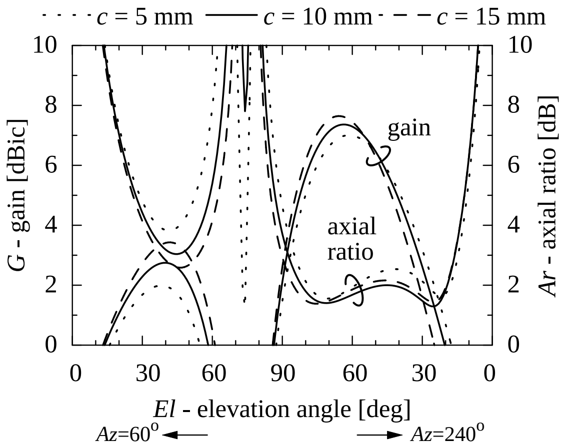

Figure 5 Gain and axial ratio versus elevation angle (patch #3 off)

Based on the above results, the distance between the tip-truncated edge and the center point of the array (*c*) is 10 mm, and the longest length of the array l_a is 150 mm. In the following analysis, the simulation and measurement results are discussed for *c* = 10 mm.

Figure 6 shows the *S* parameters (characterized by $|S_{11}|$) of the simulated result for *c* = 10 mm and element no. 3 off that is validated by measurement in the anechoic chamber. The measured result is shifted about 0.8% to the higher frequency compared to the simulated one. We surmise that during the measurement in the chamber, the system components (e.g., cables, connectors, plastic screws) affect the antenna performances (Sri Sumantyo et al., 2005b; Otero & Rojas, 1995; Lier & Jacobsen, 1983; Delgado et al., 1989; Iyer & Karekar, 1991; Maci & Borselli, 1996; Maci et al., 2000). In general, the measured result is similar to the simulated one.

Based on the results in Figure 7 for the axial ratio characteristics, the minimum axial ratio is confirmed at 0.1 dB and 0.9 dB for the simulation (*f* = 2.5125 GHz) and measurement (*f* = 2.5225 GHz), respectively. The measured axial ratio satisfies the target in the desired frequency band. The measured minimum axial ratio is slightly shifted by 0.4% to the higher frequency compared with the simulated one; this shift may be due to connectors and cables.

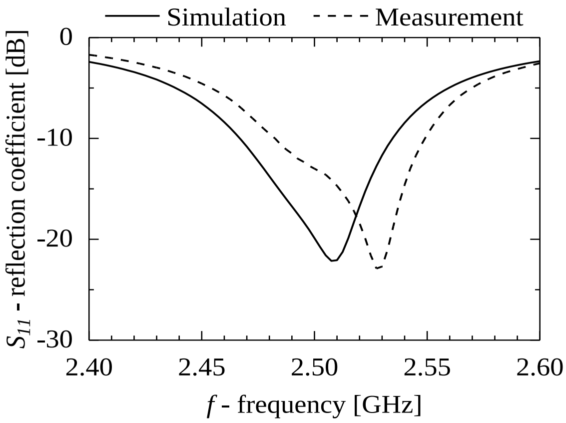

Figure 6 S parameter versus frequency

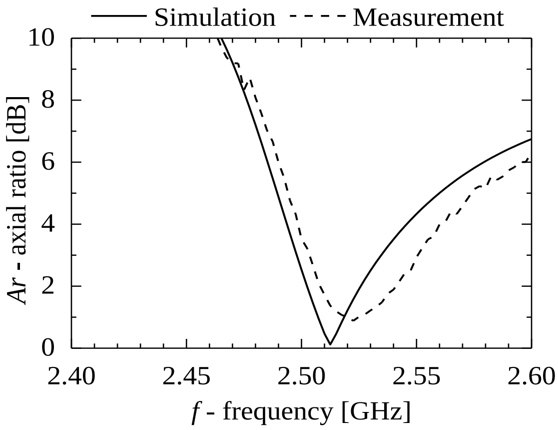

Figure 7 Axial ratio versus frequency

Figure 8 depicts the axial ratio performance in the *Az*-plane. The simulated 5-dBic gain beamwidth (at f = 2.5125 GHz) is 124° and the measured one (at f = 2.5225 GHz) is 116°. The simulated and measured 3-dB axial ratio beamwidth is 140° and 92°, respectively. We find that the simulated 5-dBic gain beamwidth and the 3-dB axial ratio meet all *Az* angles because each beam is wider than 120°. Due to the effect of the ground plane size, each measured beam coverage is less than 120°. In Section 4, the beam switching verification of the fabricated array will be discussed

The gain pattern in the *El*-plane is shown in Figure 9. The simulated 5-dBic beamwidth is 42° and the measured one is 38° when the beam peak is tilted to *El* = 64° and 62°, respectively. The side lobe is confirmed at 2.8 dBic and 4.4 dBic for the simulated and measured results, respectively. The increased side lobe level occurring due to the infinite ground size in the simulation does not occur in the measurement.

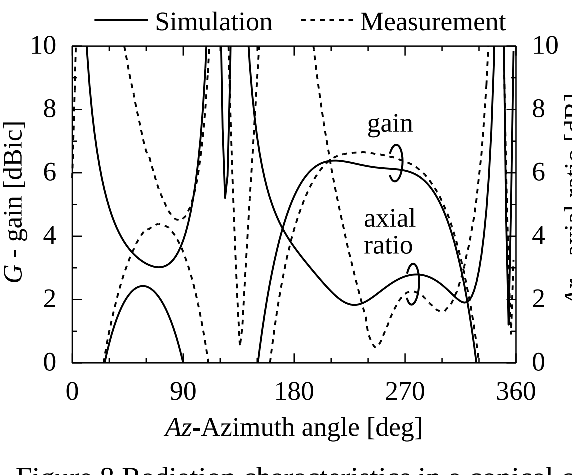

Figure 8 Radiation characteristics in a conical cut (patch #3 off, *El* = 48°)

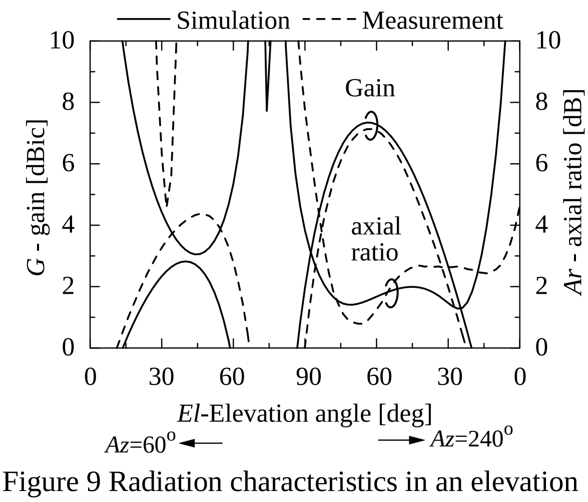

Figure 9 Radiation characteristics in an elevation cut (patch #3 off, *El* = 48°)

Because the array will be placed on a car's roof, pitch angle fluctuation must be considered. The pitch angle fluctuation, set to be about ±10° in elevation angle at the center, is *El* = 48°. In this pitch angle range, the gain and axial ratios have to satisfy a minimum gain of 5 dBic and a maximum axial ratio of 3 dB. From Fig. 9, the minimum gain for simulation is met for *El* = 40° to 82°. In addition, the measured one meets the requirement from *El* = 42° to 80°. As for the maximum axial ratio, both the simulated and measured AR at *El* = 38° to 58° are lower than the results at 3 dB. From these findings, the gain and axial ratios mainly satisfy the target even though they must be considered at a lower *El* performance.

4. BEAM SWITCHING MECHANISM VERIFICATION

The beam switching mechanism noted earlier needs to be verified. The gain and axial ratio characteristics of the beam switching is verified in the azimuthal plane by switching off one of the available three elements at El = 48°. The result is shown in Figure 10. The maximum gain is 5.1 dBic and 4.7 dBic for simulation and measurement, respectively. The simulated minimum axial ratio is 2.8 dB and the measured one is 5.5 dB. The simulated result (with infinite ground plane) meets the requirement, but the measured one (with finite ground plane) has a narrow coverage. This may be due to the different environmental models between simulation and measurement.

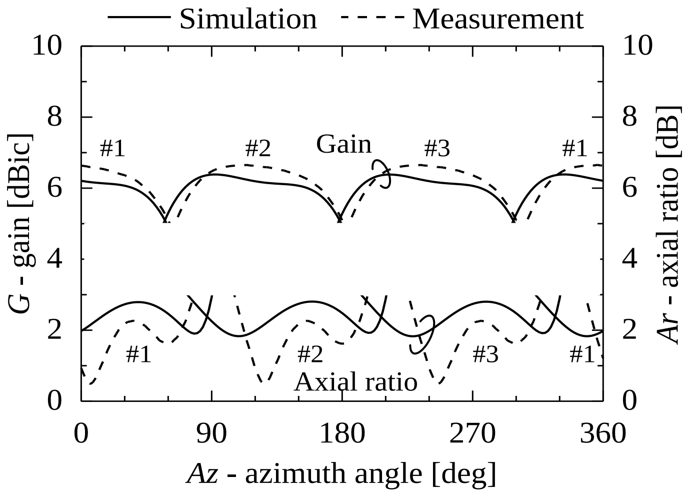

Figure 10 Switched beam characteristics in the conical-cut plane (El = 48°)

5. CONCLUSION

JAXA has launched ETS-VIII to conduct experiments on mobile satellite communications at the S-band frequency. This paper proposes a compact circularly polarized array for satellite tracking aimed at land mobile vehicle applications. The MoM-based software is applied for numerically designing the array and studying the characteristics of array performances. The array is then measured in an anechoic chamber to validate the simulation. The simulated and measured results show good performance in terms of S-parameter, gain, and axial ratios. Verification of the array's switchable beam is also confirmed.

The proposed antenna is thinner, smaller, and simpler compared to previous state-of-the-art antennas. It also has a relatively stable switchable beam to cover all azimuth angles by only three differently directed beams. In conclusion, the performance of the array meets the required specifications for installing on a land vehicle's roof.

6. ACKNOWLEDGEMENT

We thank the Antenna Laboratory, Chiba University, for providing the measurement setup during this land mobile satellite communications project.

7. REFERENCES

Alonso, J.I., Blas, J.M., Garcia, L.E., Ramos, J., de Pablos, J., Grajal, J., Gentili, G.G., Gismero, J., Perez, F., 1996. • Low Cost Electronically Steered Antenna and Receiver System for Mobile Satellite Communications, *IEEE Trans. on Microwave Theory and Techniques*, Volume 44, pp. 2438–2449

Bayer, H., Krauss, A., Stephan, R., Hein, M.A., 2014. Land-mobile Ka-band Satcom Tracking Antenna Employing a Printed Circuit Board Based Multimode Monopulse Feed, In: *2014 IEEE-APS Topical Conference on Antennas and Propagation in Wireless Communications* (APWC), pp. 296–299

Delgado, H.J., Williams, J.T., Long, S.A., 1989. Subtraction of Edge-diffracted Fields in Antenna Radiation Pattern for Simulation of Infinite Ground Plane, *Electronics Letters*, Volume 25, pp. 694–696

Fujimoto, K., James, J.R., 1994. *Mobile Antenna Systems Handbook*, Artech House, Boston, London, UK

Garg, R., Bhartia, P., Bahl, I., Ittipiboon, A., 2001. *Microstrip Antenna Design Handbook*, Artech House, Boston, Massachusetts, USA

Gatti, M.S., Nybakken, D.J., 1990. A Circularly Polarized Crossed Drooping Dipole Antenna, • *IEEE Ant. and Prop. Soc. Intl. Sym.*, Volume 1, pp. 254–257

Huang, J., Densmore, A.C., 1991. Microstrip Yagi Array Antenna for Mobile Satellite Vehicle Application, • *IEEE Trans. on Antennas and Prop.*, Volume 39, pp. 1024–1030

Ishihara, H., Yamamoto, A., Ogawa, K., 2002. A Simple Model for Calculating the Radiation Patterns of Antennas Mounted on a Vehicle Roof, In: *Proceeding Interim Int. Symp. on Antenna and Propagation.*, pp. 548–551

Ito, K., Ohmaru, K., Konishi, Y., 1988. Planar Antennas for Satellite Reception, *IEEE Trans. Broadcasting*, Volume 34(4), pp. 457–464

Iyer, S.M.V., Karekar, R.N., 1991. Edge Effects for Resonance Frequency of Covered Rectangular Microstrip Patch Antenna, *Electronics Letters*, Volume 27, pp. 1509–1511

James, J.R., Hall, P.S., 1989. *Handbook of Microstrip Antennas*, Peter Peregrinus, London, UK.

Jang, J. H., Tanaka, M., Hamamoto, N., 2002. Portable and Deployable Antenna for ETS-VIII, In: *Proceeding Interim Int. Symp. on Antenna and Propagation*, pp. 49–52

Kilgus, C.C., 1975. Shaped-conical Radiation Pattern Performance of the Backfire Quadrifilar Helix, • *IEEE Trans. Ant. Prop.*, Volume 23, pp. 392–397

Kumar, G., Ray, K.P., 2003. *Broadband Microstrip Antennas*, Artech House, Boston, Massachusetts, USA

Kuramoto, A., Yamane, T., Endo, N., 1988. • Mechanically Steered Tracking Antenna for Land Mobile Satellite Communications, • In: *Proceeding of IEEE Antennas and Propagation Society International Symposium*, Syracuse, USA, Volume 2, pp. 1314–1317

Lier, E., Jacobsen, K., 1983. Rectangular Microstrip Patch Antennas with Infinite and Finite Ground Plane Dimensions, *IEEE Trans. on Antennas and Propagat.*, Volume 31, pp. 978–984

Lu, J.H., Wong, K.L., 2002. Singly-fed Circularly Polarised Equilateral-triangular Microstrip Antenna with a Tuning Stub, *IEEE Trans. Antennas and Propagat.*, Volume 48, pp. 1869–1872

Maci, S., Borselli, L., 1996. Diffraction at the Edge of a Truncated Grounded Dielectric Slab, *IEEE Trans. on Antennas and Propagat.*, Volume 44, pp. 863–873

Maci, S., Borselli, L., Cucurachi, A., 2000. Diffraction from a Truncated Grounded Dielectric Slab: A Comparative Full-wave/Physical-optics Analysis, *IEEE Trans. on Antennas and Propagat.*, Volume 48, pp. 48–57

Nakano, H., Vichien, K., Sugiura, T., Yamauchi, J., 1990. A Singly-fed Patch Antenna Radiating a Circularly Polarised Conical Beam, • *Electronics Letters*, Volume 26(10), pp.

Ohmine, H., Sunahara, Y., Matsunaga, M., 1996. A TM_{21} Mode Annular Ring Microstrip Antenna for Personal Satellite Communication Use, • *IEICE Trans. Communications*, Volume E79-B(9), pp. 1227–1233

Ohmori, S., Wakana, H., Kawase, S., 1998. *Mobile Satellite Communications*, • Artech House, Norwood, Massachusetts, USA

Otero, M.F., Rojas, R.G., 1995. Analysis and Treatment of Edge Effects on the Radiation Pattern of a Microstrip Patch Antenna, In: *Proceeding IEEE AP-S Int. Symp.*, pp. 1050–1053

Sri Sumantyo, J.T., Ito, K., 2004a. Simple Satellite-tracking Triangular-patch Array Antenna for ETS-III applications, *IEICE Technical Report*, AP2003–236, pp. 39–44

Sri Sumantyo, J.T., Ito, K., Delaune, D., Tanaka, T., Yoshimura, H., 2004b. Simple Satellite-tracking Dual-band Triangular-patch Array Antenna for ETS-VIII applications, In: *Proceeding IEEE Int. Symp. on Antenna and Propagat.*, pp. 2500–2503

Sri Sumantyo, J.T., Ito, K., Takahashi, M., 2005a. Dual Band Circularly Polarized Equilateral Triangular Patch Array Antenna for Mobile Satellite Communications, *IEEE Trans. Antennas and Propagat.*, Volume 53(11), pp. 3477–3485

Sri Sumantyo, J.T., Ito, K., Delaune, D., Tanaka, T., Onishi, T., Yoshimura, H., 2005b. Numerical Analysis of Ground Plane Size Effects on Patch Array Antenna Characteristics for Mobile Satellite Communications, *International Journal of Numerical Modelling*, Volume18, pp. 95–106

Sri Sumantyo J.T., Ito, K., 2006. Circularly Polarised Equilateral Triangular Patch Array Antenna for Mobile Satellite Communications, In: *IEE Proceedings - Microwaves, Antennas and Propagation*, Volume 153, pp. 544–550

Suzuki, Y., Miyano, N., Chiba, T., 1987. Circularly Polarised Radiation from Singly-fed Equilateral-triangular Microstrip Antenna, In: *Proceedings IEE*, Volume 134 (Pt.H) pp. 194–198

Vaccaro, S., Tiezzi, F., Rúa, M.F., De Oro, C.D.G., 2010. Ku-band Low-profile Rx-only and Tx-Rx Antennas for Mobile Satellite Communications, In: *2010 IEEE International Symposium on Phased Array Systems and Technology* (ARRAY), pp. 536–542

Yamaguchi, R., Ebine, Y., 1997. Design of Vehicle Antenna using Helical Array for Mobile Satellite Communication System, • *Tech. Report of IEICE*, AP 97–64, pp. 35–40 (in Japanese)